

Origin of the Bite Angle Effect on Rhodium Diphosphine Catalyzed Hydroformylation

Lars A. van der Veen,[†] Peter H. Keeven,[†] Gerard C. Schoemaker,[†]
Joost N. H. Reek,[†] Paul C. J. Kamer,[†] Piet W. N. M. van Leeuwen,^{*,†}
Martin Lutz,[‡] and Anthony L. Spek[‡]

*Institute of Molecular Chemistry, University of Amsterdam, Nieuwe Achtergracht 166,
1018 WV Amsterdam, and Bijvoet Center for Biomolecular Research, Utrecht University,
Padualaan 8, 3584 CH Utrecht, The Netherlands*

Received September 20, 1999

The bite angle effect on the rhodium diphosphine catalyzed hydroformylation was investigated in detail. A series of xantphos-type ligands with natural bite angles ranging from 102° to 121° was synthesized, and the effect of the natural bite angle on coordination chemistry and catalytic performance was studied. X-ray crystal structure determinations of the complexes (nixantphos)Rh(CO)H(PPh₃) and (benzoxantphos)Rh(CO)H(PPh₃) were obtained. In contrast to the natural bite angle calculations, approximately the same diphosphine bite angles were observed in both crystal structures. The solution structures of the (diphosphine)Rh(CO)H(PPh₃) and (diphosphine)Rh(CO)₂H complexes were studied by IR and NMR spectroscopy. The spectroscopic studies showed that all (diphosphine)Rh(CO)₂H complexes exhibit dynamic equilibria between diequatorial (**ee**) and equatorial–apical (**ea**) isomers. The equilibrium compositions could not be correlated with the calculated natural bite angles. In the hydroformylation of 1-octene an increase in selectivity for linear aldehyde formation and activity was observed with increasing natural bite angle. For styrene the same trend in selectivity for the linear aldehyde was found. For the first time CO dissociation rates of (diphosphine)Rh(CO)₂H complexes were determined using ¹³CO labeling in rapid-scan high-pressure (HP) IR experiments. The observed CO dissociation rates for three complexes proved to be orders of magnitude higher than the hydroformylation rates and, contrary to the hydroformylation activity, did not reveal a correlation with the natural bite angle. These findings indicate that the bite angle effect on hydroformylation activity is dominated by the rates of reaction of the reactive, unsaturated (diphosphine)Rh(CO)H intermediates with CO and alkene. The bite angle affects the selectivity in the steps of alkene coordination and hydride migration; the structure of the saturated (diphosphine)Rh(CO)₂H complex has only some circumstantial relevance to the selectivity.

Introduction

Rhodium-catalyzed hydroformylation is one of the most prominent applications of homogeneous catalysis in industry.^{1–3} Since stereoelectronic properties of ligands, like in most catalytic systems, have a pronounced influence on the course of the rhodium-catalyzed hydroformylation, extensive research has been devoted to fine-tuning of the catalytic performance by ligand

modification. High selectivities in the hydroformylation of terminal alkenes have been reported for both diphosphine- and diphosphite-modified catalysts.^{4–9} Functionalized alkenes have been hydroformylated with high selectivity by Cuny and Buchwald using rhodium diphosphite systems.¹⁰ Stanley has developed a highly active and selective bimetallic catalyst based on tetradentate phosphine ligands.¹¹ Novel ligands for the selective linear hydroformylation of internal alkenes, which is of

[†] Department of Inorganic Chemistry and Homogeneous Catalysis, University of Amsterdam.

[‡] Department of Crystal & Structural Chemistry, Utrecht University.

(1) Parshall, G. W. *Homogeneous Catalysis: The Applications and Chemistry of Catalysis by Soluble Transition Metal Complexes*; Wiley: New York, 1980.

(2) Tolman, C. A.; Faller, J. W. In *Homogeneous Catalysis with Metal Phosphine Complexes*; Pignolet, L. H., Ed.; Plenum: New York, 1983; pp 81–109.

(3) Frohning, C. D.; Kohlpaintner, C. W. In *Applied Homogeneous Catalysis with Organometallic Compounds: A Comprehensive Handbook in Two Volumes*; Cornils, B., Herrmann, W. A., Eds.; VCH: Weinheim, 1996; Vol. 1, pp 27–104.

(4) Devon, T. J.; Phillips, G. W.; Puckette, T. A.; Stavinoha, J. L.; Vanderbilt, J. J. (to Eastman Kodak) U.S. Patent 4.694.109, 1987 [*Chem. Abstr.* **1988**, 108, 7890].

(5) Casey, C. P.; Whiteker, G. T.; Melville, M. G.; Petrovich, L. M.; Gavney, J. A., Jr.; Powell, D. R. *J. Am. Chem. Soc.* **1992**, 114, 5535–5543.

(6) Kranenburg, M.; van der Burgt, Y. E. M.; Kamer, P. C. J.; van Leeuwen, P. W. N. M. *Organometallics* **1995**, 14, 3081–3089.

(7) Billig, E.; Abatjoglou, A. G.; Bryant, D. R. (to Union Carbide) EP 213,639,1987 [*Chem. Abstr.* **1987**, 107, 7392r].

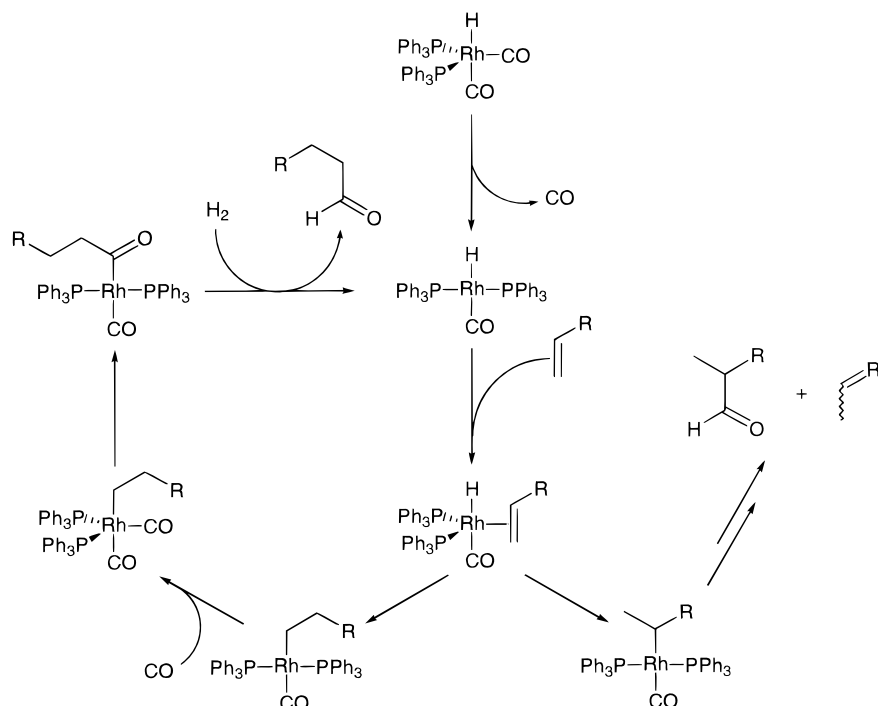
(8) van Rooy, A.; Kamer, P. C. J.; van Leeuwen, P. W. N. M.; Goubitz, K.; Fraanje, J.; Veldman, N.; Spek, A. L. *Organometallics* **1996**, 15, 835–847.

(9) Buisman, G. J. H.; van der Veen, L. A.; Klootwijk, A.; de Lange, W. G. J.; Kamer, P. C. J.; van Leeuwen, P. W. N. M.; Vogt, D. *Organometallics* **1997**, 16, 2929–2939.

(10) Cuny, G. D.; Buchwald, S. L. *J. Am. Chem. Soc.* **1993**, 115, 2066–2068.

(11) Broussard, M. E.; Juma, B.; Train, S. G.; Peng, W.-J.; Laneman, S. A.; Stanley, G. G. *Science* **1993**, 260, 1784–1788.

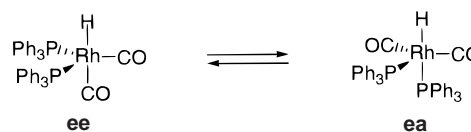
Scheme 1



great interest in both industry and synthetic organic chemistry, were developed recently.^{12,13} Systematic studies of the influence of ligand structure on catalytic performance in the hydroformylation reaction are rare, however, and despite the development of a wide variety of ligands, consistent structure–activity relationships are still lacking.¹⁴

The generally accepted mechanism for rhodium-catalyzed hydroformylation as proposed by Wilkinson in 1968 is shown in Scheme 1.¹⁵ The active catalyst is a trigonal bipyramidal hydridorhodium complex, which usually contains two phosphorus ligands. According to this mechanism, the selectivity is determined in the step that converts a five-coordinate $L_2Rh(CO)H(alkene)$ complex into either a linear or branched $L_2Rh(CO)(alkyl)$. For the linear rhodium alkyl species this step is virtually irreversible at moderate temperatures and sufficiently high pressures of CO.^{16,17} The structure of the alkene complex is therefore thought to play a crucial role in controlling regioselectivity.⁵ Contrary to the $L_2Rh(CO)_2H$ complex, the $L_2Rh(CO)H(alkene)$ complex has never been observed directly. Brown and Kent have shown that the PPh_3 -modified $L_2Rh(CO)_2H$ complex consists of two rapidly equilibrating isomeric structures in which the phosphine ligands coordinate in a diequatorial (**ee**) and an equatorial–apical (**ea**) fashion.^{18,19} Previous studies on electronically modified diphosphine

ligands have demonstrated that similar dynamic equilibria between **ee** and **ea** complex isomers also exist for diphosphine ligands.^{14,20} The **ee:ea** isomer ratio of the complexes proved to be strongly dependent on phosphine basicity; the **ee:ea** ratio increases with decreasing phosphine basicity.



As a result of their extensive use in catalysis, the influence of phosphine structure on catalytic performance has been studied in great detail.²¹ Tolman introduced the concept of cone angle θ and the electronic parameter χ as measures of respectively the steric bulk and the electronic properties of phosphorus ligands.^{22,23} Casey and Whiteker developed the concept of the natural bite angle as an additional characteristic of diphosphine ligands based on molecular mechanics calculations.²⁴ The pronounced influence of the natural bite angle of diphosphine ligands on activity and selectivity has been shown for several catalytic reactions.^{5,6,25–27}

How the bite angle affects the activity and selectivity in the rhodium diphosphine catalyzed hydroformylation

(12) Burke, P. M.; Garner, J. M.; Tam, W.; Kreutzer, K. A.; Teunissen, A. J. J. M. (to DSM/Du Pont de Nemours) WO 97/33854, 1997 [*Chem. Abstr.* **1997**, 127, 294939r].

(13) van der Veen, L. A.; Kamer, P. C. J.; van Leeuwen, P. W. N. M. *Angew. Chem., Int. Ed.* **1999**, 38, 336–338.

(14) Casey, C. P.; Paulsen, E. L.; Beuttenmueller, E. W.; Proft, B. R.; Petrovich, L. M.; Matter, B. A.; Powell, D. R. *J. Am. Chem. Soc.* **1997**, 119, 11817–11825.

(15) Evans, D.; Osborn, J. A.; Wilkinson, G. *J. Chem. Soc. (A)* **1968**, 3133–3142.

(16) Lazzaroni, R.; Uccello-Barretta, G.; Benetti, M. *Organometallics* **1989**, 8, 2323–2327.

(17) Casey, C. P.; Petrovich, L. M. *J. Am. Chem. Soc.* **1995**, 117, 6007–6014.

(18) Brown, J. M.; Kent, A. G. *J. Chem. Soc., Perkin Trans. 2* **1987**, 1597–1607.

(19) Throughout this work, notations **ee** and **ea** refer to respectively the diequatorial and the equatorial–apical chelation modes of the diphosphines in trigonal bipyramidal complexes.

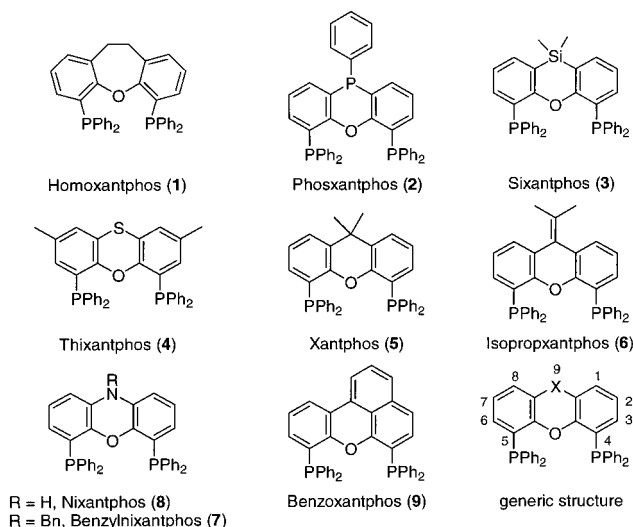
(20) van der Veen, L. A.; Boele, M. D. K.; Bregman, F. R.; Kamer, P. C. J.; van Leeuwen, P. W. N. M.; Goubitz, K.; Fraanje, J.; Schenk, H.; Bo, C. *J. Am. Chem. Soc.* **1998**, 120, 11616–11626.

(21) Beller, M.; Cornils, B.; Frohning, C. D.; Kohlpaintner, C. W. *J. Mol. Catal. A: Chem.* **1995**, 104, 17–85.

(22) Tolman, C. A. *Chem. Rev.* **1977**, 77, 313–348.

(23) Tolman, C. A. *J. Am. Chem. Soc.* **1970**, 92, 2953–2956.

(24) Casey, C. P.; Whiteker, G. T. *Isr. J. Chem.* **1990**, 30, 299–304.

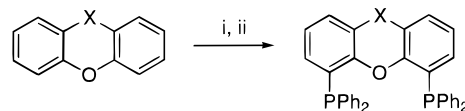
**Figure 1.** The xantphos ligands.**Table 1.** Calculated Natural Bite Angle and Flexibility Range for the Xantphos Ligands

ligand	X	β_n , ^a deg	flexibility range, ^a deg
homoxantphos (1)	CH ₂ -CH ₂	102.0	92-120
phosxantphos (2)	PPh	107.9	96-127
sixantphos (3)	Si(CH ₃) ₂	108.5	96-130
thixantphos (4)	S	109.6	96-133
xantphos (5)	C(CH ₃) ₂	111.4	97-133
isopropoxantphos (6)	C=C(CH ₃) ₂	113.2	98-139
benzylnixantphos (7)	NBn	114.1	99-139
nixantphos (8)	NH	114.2	99-141
benzoxantphos (9)	fused benzene ring	120.6	102-146

^a The natural bite angle (β_n) and the flexibility range were calculated as by Casey and Whiteker.²⁴ β_n is defined as the preferred chelation angle determined only by ligand backbone constraints and not by metal valence angles. The flexibility range is defined as the accessible range of bite angles within 3 kcal mol⁻¹ excess strain energy from the calculated natural bite angle.

is still not understood in detail.¹⁴ To investigate the exact influence of the natural bite angle of diphosphine ligands on catalytic performance and coordination chemistry in rhodium complexes, we have developed a new family of diphosphine ligands based on xanthene-type backbones.⁶ Variation of the substituent at the 9-position of the generic backbone structure enables the construction of a series of diphosphine ligands having a wide range of natural bite angles (Figure 1, Table 1). Moreover, the backbone structure in this type of ligand ensures that mutual variation in electronic properties and in steric size within the series of ligands is minimal. We have previously reported on the first members of this new family of ligands (sixantphos (3), thixantphos (4), and xantphos (5)), and we have shown that relatively wide natural bite angles give rise to high selectivities and activities in the rhodium-catalyzed hydroformylation.⁶ On the basis of these results and the work of Casey and co-workers, we hypothesized that there is a regular increase in selectivity for linear aldehyde formation with increasing natural bite angle in the family of xantphos ligands.⁵

Here we report the synthesis of new members of the xantphos series, their coordination chemistry, and their catalytic performance in the rhodium-catalyzed hydroformylation. In this series of ligands there is an almost regular increase in hydroformylation activity and se-

Scheme 2^a

^a (i) *n*-BuLi/TMEDA/Et₂O/0-25 °C; (ii) PPh₂Cl/hexanes/0-25 °C.

lectivity with increasing natural bite angle. No clear correlation between the chelation mode and the natural bite angle was found in the (diphosphine)Rh(CO)₂H complexes. To obtain a better understanding of how the bite angle affects the hydroformylation activity, we have developed a method to measure the CO dissociation rates of (diphosphine)Rh(CO)₂H complexes. By using ¹³C labeling in rapid-scan high-pressure (HP) IR experiments we were able to determine the rate constants for three (diphosphine)Rh(CO)₂H complexes.

Results

Synthesis. Ligands 1-9 were all synthesized by selective dilithiation of the appropriate heterocycle, followed by reaction with chlorodiphenylphosphine (Scheme 2). 10,11-Dihydrodibenzo[*b*,*f*]oxepine,²⁸ 10-phenylphenoxaphosphine,²⁹ 10-(*tert*-butyldimethylsilyl)phenoxazine,³⁰ and benzo[*k*,*l*]xanthene³¹ were prepared according to literature procedures. 10-Isopropylidene-xanthene (10) was synthesized by a McMurry reaction³² starting from xanthone and acetone. In the synthesis of phosxantphos (2) phenyllithium was used as metalating agent instead of *n*-butyllithium to annihilate side product formation by competing nucleophilic substitution at the ring phosphorus atom by the lithiating agent.³³ Benzylnixantphos (7) was obtained by deprotonation of nixantphos (8) with sodium hydride followed by reaction with benzyl chloride. Typical yields of the ligands varied from 62% for phosxantphos (2) to 80% for homoxantphos (1) based on heterocyclic starting material. Table 1 shows the effect of the heterocyclic backbone on the calculated natural bite angle and flexibility range of the ligands. Comparison of the carbonyl frequencies of the (diphosphine)Rh(CO)₂H complexes (vide infra) reveals that the electronic effect of the backbone on the electron density on the rhodium center is marginal, proving that the ligands are electronically very similar. Therefore, this series of ligands is ideally suited for studying only the influence of the natural bite angle in catalysis.

As was pointed out by a reviewer, it should be noted that xantphos 1 is not completely isostructural to the

(25) Kranenburg, M.; Kamer, P. C. J.; Vogt, D.; van Leeuwen, P. W. N. M. *J. Chem. Soc., Chem. Commun.* **1995**, 2177-2178.

(26) Kranenburg, M.; Kamer, P. C. J.; van Leeuwen, P. W. N. M. *Eur. J. Inorg. Chem.* **1998**, 25-27.

(27) Kamer, P. C. J.; Reek, J. N. H.; van Leeuwen, P. W. N. M. *CHEMTECH* **1998**, 28, 27-33.

(28) Hess, B. A., Jr.; Bailey, A. S.; Bartusek, B.; Boekelheide, V. J. *Am. Chem. Soc.* **1969**, 91, 1665-1672.

(29) Schlosser, M. In *Organometallics in Synthesis: A Manual*; Schlosser, M., Ed.; Wiley: Chichester, 1994; p 115.

(30) Antonia, Y.; Barrera, P.; Contreras, O.; Franco, F.; Galeazzi, E.; Garcia, J.; Greenhouse, R.; Guzmán, A.; Velarde, E.; Muchowski, J. M. *J. Org. Chem.* **1989**, 54, 2159-2165.

(31) Orchin, M. *J. Am. Chem. Soc.* **1948**, 70, 495-497.

(32) McMurry, J. E.; Krepski, L. R. *J. Org. Chem.* **1976**, 41, 3929-3930.

(33) Levy, J. B.; Walton, R. C.; Olsen, R. E.; Symmes, C. J. *Phosphorus, Sulfur* **1996**, 109-110, 545-548.

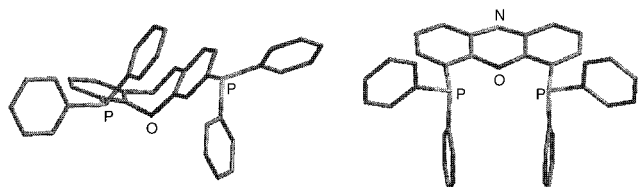


Figure 2. Wire models of the minimized structures of xantphos **1** (left) and xantphos **8** (right).

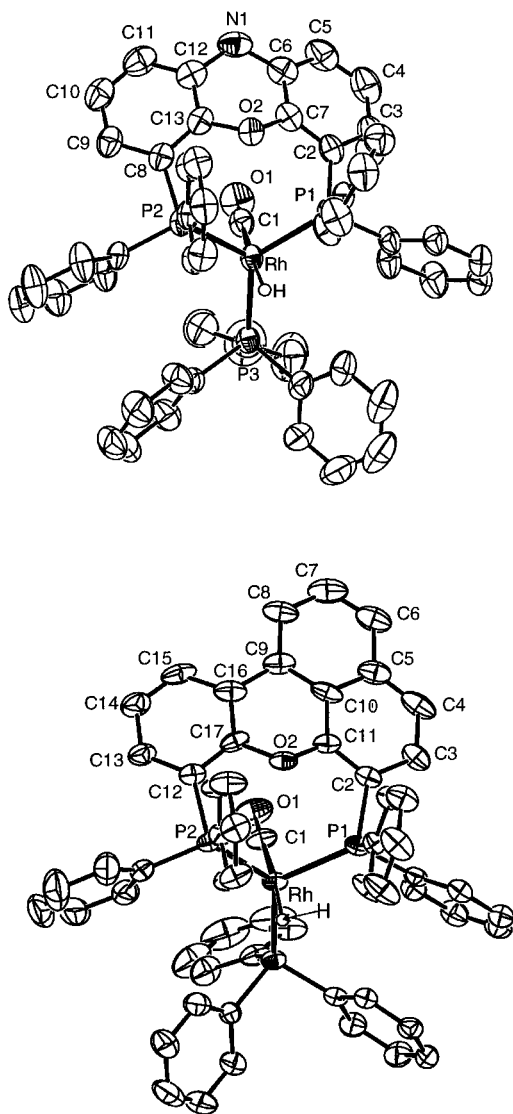


Figure 3. Crystal structures and numbering schemes for (nixantphos)Rh(CO)H(PPh₃) (**18a**) (top) and (benzoxantphos)Rh(CO)H(PPh₃) (**19a**) (bottom) (non-hydride hydrogen atoms have been omitted for clarity). Displacement ellipsoids are shown at 50% probability.

other xantphos ligands. With respect to the disposition of the diphenylphosphine moieties, the conformations of the xantphos ligands **2–9** can roughly be described as pseudo-*C_s* (Figure 2 and see also the crystal structures in Figure 3). Since the backbone of ligand **1** is based on a seven-membered ring instead of a six-membered one, the diphenylphosphine moieties of this ligand adopt a different conformation that can be called pseudo-*C₂* (Figure 2). These structural differences between xantphos **1** and the other xantphos ligands may have some effect on the coordination chemistry and catalytic performance of this ligand. The natural bite

Table 2. Selected Bond Lengths and Angles for (Nixantphos)Rh(CO)H(PPh₃) (**18a**) and (Benzoxantphos)Rh(CO)H(PPh₃) (**19a**)

(nixantphos)Rh(CO)H(PPh ₃) (18a)	(benzoxantphos)Rh(CO)H(PPh ₃) (19a)		
Bond Lengths (Å)			
Rh–P(1)	2.3288(7)	Rh–P(1)	2.3616(16)
Rh–P(2)	2.3408(7)	Rh–P(2)	2.3268(15)
Rh–P(3)	2.2854(8)	Rh–P(3)	2.2822(15)
Rh–C(1)	1.887(3)	Rh–C(1)	1.895(6)
Rh–H	1.65(3)	Rh–H	1.62(6)
Bond Angles (deg)			
P(1)–Rh–P(2)	110.21(3)	P(1)–Rh–P(2)	109.16(5)
P(1)–Rh–P(3)	125.12(3)	P(1)–Rh–P(3)	118.45(5)
P(2)–Rh–P(3)	120.98(3)	P(2)–Rh–P(3)	129.07(6)
P(1)–Rh–C(1)	93.49(8)	P(1)–Rh–C(1)	97.9(2)
P(2)–Rh–C(1)	97.88(9)	P(2)–Rh–C(1)	93.1(2)
P(3)–Rh–C(1)	97.70(9)	P(3)–Rh–C(1)	97.15(19)

angle calculations indicate, however, that in the rhodium complexes the diphenylphosphine moieties of xantphos **1** conform to the same pseudo-*C_s* symmetry as the other xantphos ligands.

(Diphosphine)Rh(CO)H(PPh₃) Complexes 11a–19a. To investigate the effect of the natural bite angle on chelation behavior, the structures of the (diphosphine)Rh(CO)H(PPh₃) complexes and the (diphosphine)-Rh(CO)₂H complexes of all xantphos ligands were studied in detail.³⁴ Formation of the (diphosphine)Rh(CO)H(PPh₃) complexes was easily accomplished by displacement of PPh₃ in (PPh₃)₃Rh(CO)H on the addition of diphosphines **1–9**.⁵⁶ Crystals of the (diphosphine)Rh(CO)H(PPh₃) complexes suitable for crystal structure determinations were obtained for ligands **8** and **9**.

The X-ray crystal structures of (nixantphos)Rh(CO)H(PPh₃) (**18a**) and (benzoxantphos)Rh(CO)H(PPh₃) (**19a**) are shown in Figure 3. Selected bond lengths and angles of complexes **18a** and **19a** are given in Table 2. Both crystal structures reveal distorted trigonal bipyramidal complex geometries with all the phosphines occupying equatorial sites. The Rh atom is located slightly above the equatorial plane defined by the three phosphorus atoms and displaced toward the apical carbonyl ligand. The positions of the hydride ligands were determined from difference Fourier maps. These positions are not accurate, but ¹H NMR spectroscopy also indicates that the hydrides occupy the apical sites trans to the carbonyl ligands (vide infra).

The observed P–Rh–P bite angles for ligands **8** and **9** in the crystal structures are 110.21(3)° and 109.16(5)°, respectively. The observed bite angles are within the flexibility ranges calculated for the ligands and close to the bite angle observed in the complex containing ligand **4** (111.73(5)°).²⁰ The bite angle of approximately 110° found in all three crystal structures is probably the result of stereoelectronic interactions between the diphosphine and the large triphenylphosphine ligand. Furthermore, the crystal structures show several possibilities for π–π-stacking interactions between the different phenyl moieties, which could also influence the final complex geometry.

Ligands **1** and **3–9** form similar (diphosphine)Rh(CO)H(PPh₃) complexes in solution. The presence of the

(34) The complexes with diphosphines **3–5** were already described by Kranenburg et al.⁶

Table 3. Selected IR Data for (Diphosphine)Rh(CO)H(PPh₃) Complexes^a

complex	β_n , deg	ν^1 , cm ⁻¹	ν^2 , cm ⁻¹
11a	102.0	1982 (vs)	1921 (w)
12a	107.9	1966 (s)	1925 (m)
13a^b	108.5	1997 (vs)	1911 (w)
14a	109.6	1999 (vs)	1922 (w)
15a^b	111.4	1997 (vs)	1910 (m)
16a	113.2	1990 (vs)	1920 (m)
17a	114.1	2000 (vs)	1920 (m)
18a	114.2	1988 (vs)	1920 (m)
19a	120.6	1989 (vs)	1919 (m)

^a In KBr, carbonyl region. ^b In benzene.⁶

hydride ligand in the complexes is confirmed by ¹H NMR. The rhodium hydride signals appear as broad quartets or triplets of doublets at $\delta = -9.05$ to -9.23 (td, ²*J*(P,H) = 12–20 Hz). The rhodium–hydride coupling constants could not be resolved. The low values of the phosphorus–hydride coupling constants indicate that the hydrides occupying apical sites that are cis to three equatorial phosphines in distorted trigonal bipyramidal complexes. The ³¹P{¹H} NMR spectra show that in all complexes, except in that of ligand **9**, the two phosphine moieties of the diphosphine are equivalent. In the complex containing ligand **9** the two phosphorus atoms of the diphosphine are intrinsically inequivalent. In the ³¹P{¹H} NMR spectrum their signals appear in a complex ABCX pattern with a diphosphine P–P coupling constant of 77 Hz. The diphosphine P–PPh₃ coupling constants (²*J*(P,P) = 118–143 Hz) for all complexes are in agreement with structures in which all phosphines occupy equatorial sites.

For complex (**2**)Rh(CO)H(PPh₃) only very broad signals were observed in the ¹H and ³¹P{¹H} NMR spectra, even at 213 K. This is probably due to the formation of oligomeric complexes in solution via the displacement of triphenylphosphine by the phosphine moiety in the ligand backbone. The presence of a hydride and a carbonyl ligand in this complex is confirmed by IR spectroscopy. The IR spectra of complexes **11a**–**19a** in KBr all have two absorption bands in the carbonyl region due to combination bands of ν_{RhH} and ν_{CO} (Table 3).

NMR Data for (Diphosphine)Rh(CO)₂H Complexes 11b–19b. The (diphosphine)Rh(CO)₂H complexes, the resting state of the catalyst under hydroformylation conditions,²⁰ were prepared in situ from Rh(CO)₂(acetylacetonate) (acac) and diphosphine under an atmosphere of CO/H₂ (1:1). For all diphosphine ligands the formation of the (diphosphine)Rh(CO)₂H complexes was evidenced by ³¹P{¹H} and ¹H NMR spectroscopy.⁵⁷ The ³¹P{¹H} NMR spectra of the complexes with ligands **1**–**8** show a characteristic doublet at 19–25 ppm, and in the ¹H NMR spectra the rhodium hydride signal appears as an apparent triplet of doublets. In the NMR spectra of the complex (**9**)Rh(CO)₂H a double doublet is observed in the ³¹P{¹H} spectrum and a double double doublet in the ¹H spectrum due to the inequivalence of the two phosphorus atoms of the ligand. For all (diphosphine)Rh(CO)₂H complexes the characteristic heteronuclear coupling constants are depicted in Table 4.

It was shown previously that the (diphosphine)Rh(CO)₂H complexes consist of mixtures of **ee** and **ea** isomers that are in dynamic equilibrium.^{18,20} The **ee**:

Table 4. Selected NMR Data for (Diphosphine)Rh(CO)₂H Complexes^a

complex	β_n , deg	¹ <i>J</i> (Rh,H), Hz	¹ <i>J</i> (Rh,P), Hz	² <i>J</i> _{av} (P,H), Hz	ee:ea ratio ^b
11b	102.0	9.5	120	37.7	3:7
12b	107.9	7.0	127	17.0	7:3
13b	108.5	7.7	124	22.7	6:4
14b	109.6	6.6	128	14.7	7:3
15b	111.4	6.7	126	16.6	7:3
16b	113.2	6.2	128	13.0	8:2
17b	114.1	6.1	127	14.5	7:3
18b	114.2	6.0	128	13.0	8:2
19b	120.6	7.1	122	18.3/24.8 ^c	6:4

^a In C₆D₆ at 298 K. ^b Calculated from the ²*J*_{av}(P,H) using a trans ²*J*(P,H) = 106 Hz and cis ²*J*(P,H) ≤ ±2 Hz. ^c ²*J*_{av}(P,H) = 21.6 Hz.

ea isomer ratios of these mixtures were estimated using the averaged phosphorus–proton (²*J*(P,H)) coupling constants.^{14,35} Although ligand **1** has the narrowest natural bite angle and the lowest **ee:ea** isomer ratio, analysis of the whole series of (diphosphine)Rh(CO)₂H complexes reveals that there is no clear correlation between the **ee:ea** isomer ratio and the natural bite angle. Despite a difference in natural bite angles of more than 12°, the **ee:ea** ratios of the complexes containing ligands **3** ($\beta_n = 108.5^\circ$) and **9** ($\beta_n = 120.6^\circ$) are approximately the same (6:4). The low **ee:ea** isomer ratio of the complex containing ligand **9** can be the result of the high rigidity of the ligand backbone induced by the naphthyl ring. The inequivalence of the two phosphorus atoms in ligand **9** could also influence the complex mixture composition. Casey and co-workers have reported that electronically dissymmetric DIPHOS derivatives show an enhanced preference for **ea** coordination with the least basic phosphine in the equatorial position.³⁶ The relatively high **ee:ea** isomer ratio (7:3) in the complexes with ligands **2** and **4** can be attributed to the electron-withdrawing capacities of respectively the phosphorus moiety ($\sigma_m(\text{PPh}_2) = 0.11$ ³⁷) and the sulfur moiety ($\sigma_m(\text{SPh}) = 0.23$ ³⁷) in the ligand backbones.²⁰

HP IR Data for (Diphosphine)Rh(CO)₂H Complexes 11b–19b. The existence of **ee** and **ea** complex isomers was clearly evidenced by HP IR spectroscopy. The spectra of the (diphosphine)Rh(CO)₂H complexes all showed four absorption bands in the carbonyl region, which can be assigned to an **ee** and an **ea** isomer (Table 5).²⁰ The relative intensities of the absorption bands are in good agreement with the **ee:ea** ratios determined by NMR spectroscopy. Comparison of the IR frequencies shows that all bands are within a close range, indicating that the electronic properties of the ligands are similar. Despite the fact that the electronic properties of the ligand backbone have hardly any effect on the IR frequencies, they seem to have an influence on the **ee:ea** isomer ratio, as is also evidenced by the IR spectra. This implies that the composition of the (diphosphine)Rh(CO)₂H complex mixture is sensitive to small changes in ligand structure.

Hydroformylation of 1-Octene. The hydroformylation of 1-octene was carried out at 80 °C and 20 bar

(35) Yagupsky, G.; Wilkinson, G. *J. Chem. Soc. (A)* **1969**, 725–733.
 (36) Casey, C. P.; Paulsen, E. L.; Beuttenmueller, E. W.; Proft, B. R.; Matter, B. A.; Powell, D. R. *J. Am. Chem. Soc.* **1999**, *121*, 63–70.
 (37) Hansch, C.; Leo, A.; Taft, R. W. *Chem. Rev.* **1991**, *91*, 165–195.

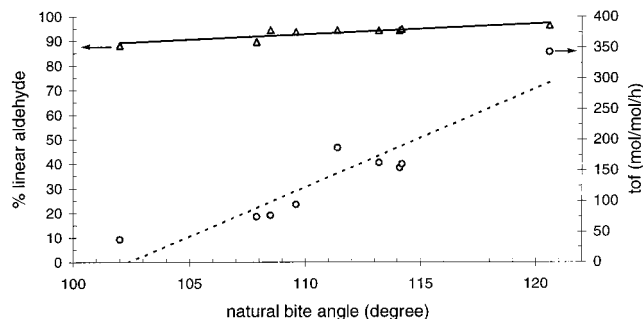
Table 5. Selected HP IR Data for (Diphosphine)Rh(CO)₂H Complexes^a

complex	β_n , deg	ν^1 , cm ⁻¹	ν^2 , cm ⁻¹	ν^3 , cm ⁻¹	ν^4 , cm ⁻¹
11b	102.0	2040 (m)	1997 (m)	1974 (m)	1951 (s)
12b	107.9	2040 (s)	1999 (m)	1977 (s)	1953 (s)
13b^b	108.5	2036 (s)	1990 (m)	1966 (m)	1940 (vs)
14b	109.6	2040 (s)	1999 (m)	1977 (s)	1953 (s)
15b^b	111.4	2036 (s)	1991 (s)	1969 (vs)	1941 (vs)
16b	113.2	2041 (s)	1999 (m)	1976 (s)	1952 (s)
17b	114.1	2038 (s)	1997 (m)	1977 (s)	1951 (s)
18b	114.2	2035 (s)	1996 (m)	1976 (s)	1949 (s)
19b	120.6	2036 (m)	1996 (m)	1976 (s)	1949 (s)

^a In cyclohexane at 80 °C and 20 bar CO/H₂ (1:1), carbonyl region.^b In benzene.⁶**Table 6. Results of the Hydroformylation of 1-Octene at 80 °C^a**

ligand	β_n , deg	l:b ratio ^b	% linear aldehyde ^b	% isomer ^b	tof ^{b,c}
1	102.0	8.50 ± 0.16	88.2 ± 0.4	1.4 ± 0.3	36.9 ± 4.8
2	107.9	14.6 ± 0.9	89.7 ± 0.4	4.2 ± 0.1	74.2 ± 1.6
3	108.5	34.3 ± 0.6	94.4 ± 0.2	2.9 ± 0.2	76.5 ± 8.8
4	109.6	56.6 ± 0.2	93.7 ± 0.1	4.7 ± 0.03	94.1 ± 0.4
5	111.4	52.2 ± 1.4	94.5 ± 0.2	3.7 ± 0.2	187 ± 4
6	113.2	49.8 ± 0.3	94.3 ± 0.1	3.8 ± 0.1	162 ± 7
7	114.1	50.6 ± 1.3	94.3 ± 0.3	3.9 ± 0.3	154 ± 12
8	114.2	69.4 ± 3.2	94.9 ± 0.4	3.7 ± 0.5	160 ± 5
9	120.6	50.2 ± 0.4	96.5 ± 0.04	1.6 ± 0.02	343 ± 7

^a Conditions: CO/H₂ = 1, P(CO/H₂) = 20 bar, ligand/Rh = 5, substrate/Rh = 637, [Rh] = 1.00 mM in toluene, number of experiments = 3. In none of the experiments was hydrogenation observed. ^b Linear over branched ratio, percent linear aldehyde, percent isomerization to 2-octene, and turnover frequency were determined at 20% alkene conversion. ^c Turnover frequency = (mol of aldehyde) (mol of Rh)⁻¹ h⁻¹.

**Figure 4.** Percentage linear aldehyde (triangles) and tof (circles) vs the calculated natural bite angle (β_n) in the hydroformylation of 1-octene (data from Table 6).

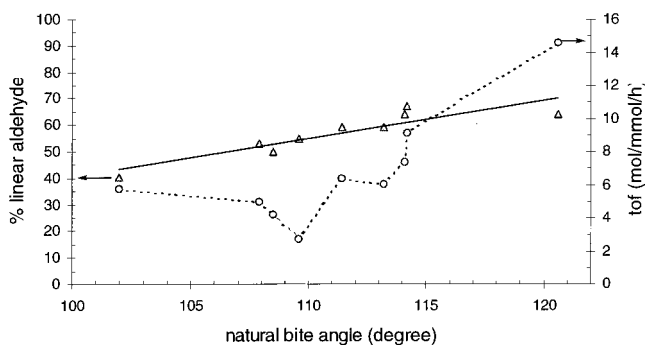
of 1:1 CO/H₂ using a 1.0 mM solution of rhodium diphosphine catalyst prepared from Rh(CO)₂(acac) and 5 equiv of ligand. The production of octene isomers, nonanal, and 2-methyloctanal was monitored by gas chromatography. The results of the experiments with ligands 1–9 are shown in Table 6 and Figure 4. Averaged turnover frequencies were determined at 20% conversion.

In the series of xantphos ligands both the selectivity for linear aldehyde formation and the rate of the reaction increase with increasing natural bite angle. Changing the natural bite angle from 102° for ligand 1 to 121° for ligand 9 results in an increase of the selectivity for linear nonanal from 88% to 97%. Moreover, a rate enhancement of almost an order of magnitude is observed. The relatively low activities of ligands 7 and 8 compared to ligand 5 can be explained by the electron-donating capacity of the nitrogen moiety (σ_m -

Table 7. Results of the Hydroformylation of Styrene at 120 °C^a

ligand	β_n , deg	l:b ratio ^b	% linear aldehyde ^b	tof ^{b,c}
1	102.0	0.68 ± 0.01	40.4 ± 0.6	5766 ± 696
2	107.9	1.13 ± 0.02	53.0 ± 0.5	4960 ± 392
3	108.5	0.99 ± 0.01	49.8 ± 0.4	4240 ± 132
4	109.6	1.22 ± 0.11	54.9 ± 2.3	2735 ± 203
5	111.4	1.45 ± 0.01	59.1 ± 0.2	6384 ± 322
6	113.2	1.45 ± 0.02	59.1 ± 0.3	6010 ± 151
7	114.1	1.78 ± 0.05	64.1 ± 0.6	7386 ± 701
8	114.2	2.04 ± 0.06	67.0 ± 0.7	9148 ± 655
9	120.6	1.78 ± 0.07	64.1 ± 0.8	14602 ± 1750

^a Conditions: CO/H₂ = 1, P(CO/H₂) = 10 bar, ligand/Rh = 10, substrate/Rh = 1746, [Rh] = 0.50 mM in toluene, number of experiments = 3. In none of the experiments was hydrogenation observed. ^b Linear over branched ratio, percent linear aldehyde, and turnover frequency were determined at 20% alkene conversion. ^c Turnover frequency = (mol of aldehyde) (mol of Rh)⁻¹ h⁻¹.

**Figure 5.** Percentage linear aldehyde (triangles) and tof (circles) vs the calculated natural bite angle (β_n) in the hydroformylation of styrene (data from Table 7).

(NH₂) = -0.16³⁷) in both backbones.²⁰ The increased flexibility of ligands 7 and 8 caused by the low barrier of inversion at nitrogen could also affect the activity.

Hydroformylation of Styrene. The hydroformylation of styrene was carried out at 120 °C and 10 bar of 1:1 CO/H₂ using a 0.50 mM solution of rhodium diphosphine catalyst prepared from Rh(CO)₂(acac) and 10 equiv of ligand. For styrene usually a distinct preference for the formation of the branched aldehyde is observed due to the stability of the benzylic rhodium species, induced by the formation of a stable η^3 complex.² The formation of the linear aldehyde can be enhanced by using high temperature and low pressure.^{6,38} The production of 1-phenylpropionaldehyde and 2-phenylpropionaldehyde was monitored by gas chromatography. The results of the experiments with ligands 1–9 are depicted in Table 7 and Figure 5. Average turnover frequencies were determined at 20% conversion.

In contrast to our findings in the hydroformylation of 1-octene, no clear trend in activity was observed in the hydroformylation of styrene. Increasing the natural bite angle from 102° to 110° results in a decrease of the hydroformylation rate, with a minimum activity observed for ligand 4. Upon a further increase of the natural bite angle to 121°, the rates increase again to result in a maximum activity observed for ligand 9.

The linear over branched ratio (l:b) and hence the selectivity for 1-phenylpropionaldehyde do increase with increasing natural bite angle, resulting in an almost

(38) Lazzaroni, R.; Raffaelli, A.; Settambolo, R.; Bertozzi, S.; Vitulli, G. *J. Mol. Catal.* **1989**, *50*, 1–9.

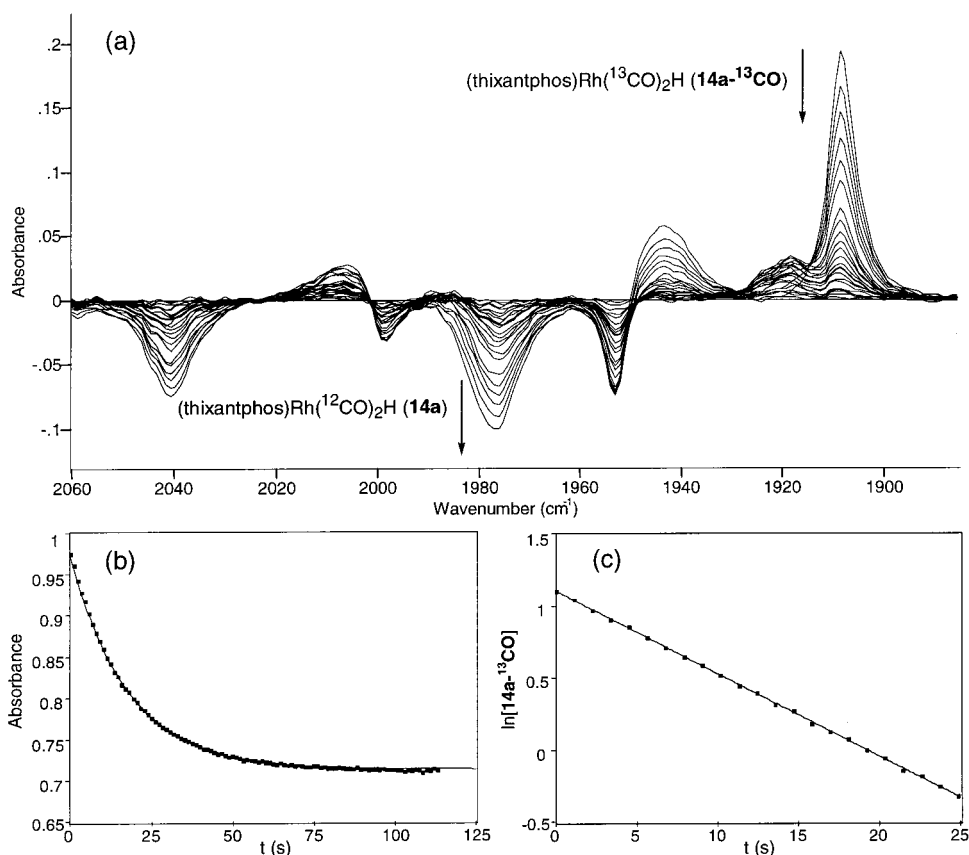


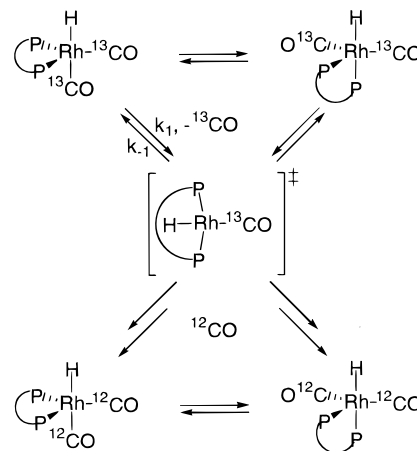
Figure 6. Representative difference IR spectrum (a) and kinetic data (b and c) for the ^{13}CO dissociation from (thixantphos)- $\text{Rh}(^{13}\text{CO})_2\text{H}$ (**14a- ^{13}CO**) in the presence of unlabeled CO at 40°C .

3-fold higher l:b ratio for ligand **8** compared to ligand **1**. Apparently, in the hydroformylation of styrene the selectivity-determining step remains the same, while the rate is probably influenced by more than one step in the catalytic cycle going from narrow to wide natural bite angles.

Kinetics of ^{13}CO Dissociation from (Diphosphine) $\text{Rh}(^{13}\text{CO})_2\text{H}$ Complexes. The hydroformylation results of both 1-octene and styrene (vide supra) clearly show that the natural bite angle has a pronounced influence on the rate of the reaction. From previous work and preliminary kinetic experiments it is clear that the rate-determining step in the hydroformylation of 1-octene with xantphos-type ligands is in an early stage in the catalytic cycle.^{20,39} CO dissociation, alkene coordination, and/or alkene insertion must be rate-limiting. So far, no reports have appeared in the literature in which the separate rate constants for these reactions are determined. We now have developed an experimental setup that enables us to obtain the rate constants for CO dissociation from the (diphosphine)- $\text{Rh}(\text{CO})_2\text{H}$ complexes. We found that by changing the common ^{12}CO ligands for isotopically pure ^{13}CO ligands, the carbonyl absorptions in the IR spectra of the (diphosphine) $\text{Rh}(\text{CO})_2\text{H}$ complexes shift $30\text{--}40\text{ cm}^{-1}$ to lower energy. Fortunately, the frequencies shift in such a way that the absorption bands of the ^{13}CO -labeled complexes are clearly separated from the ones of the

(39) Preliminary kinetic experiments with ligand **4** have shown a first-order dependence of the hydroformylation rate on both the rhodium and the alkene concentration, an approximately linear inverse dependence on the CO pressure, and no correlation with the H_2 pressure (see Supporting Information).

Scheme 3



unlabeled ^{12}CO complexes (Figure 6a). Therefore, it is possible to observe both complexes individually in IR experiments.

The rate constants k_1 (Scheme 3) for the dissociation of ^{13}CO from the (diphosphine) $\text{Rh}(^{13}\text{CO})_2\text{H}$ complexes can be determined by monitoring the exchange of ^{13}CO for ^{12}CO . This exchange can be accomplished by exposing the ^{13}CO -labeled complexes to a large excess of ^{12}CO , so any dissociated ^{13}CO will be replaced quantitatively by ^{12}CO . This will first result in the formation of the (diphosphine) $\text{Rh}(^{13}\text{CO})(^{12}\text{CO})\text{H}$ complex⁴⁰ and eventually lead to the (diphosphine) $\text{Rh}(^{12}\text{CO})_2\text{H}$ complex. The large excess of ^{12}CO prevents re-formation of (diphosphine)- $\text{Rh}(^{13}\text{CO})_2\text{H}$ by the k_{-1} pathway.

It is commonly accepted that CO exchange in (diphosphine)Rh(CO)₂H complexes proceeds via the dissociative pathway (Scheme 3).² This implies that the rate of CO dissociation should be independent of CO partial pressure and that the reaction follows simple first-order kinetics when the occurrence of the reverse reaction, ¹³CO association, is prevented.⁴¹ As a result, the overall rate equation for the reaction simplifies to eq 1 and the first-order integrated rate law eq 2.

$$-d[(\text{diphosphine})\text{Rh}(\text{}^{13}\text{CO})_2\text{H}]/dt = k_1[(\text{diphosphine})\text{Rh}(\text{}^{13}\text{CO})_2\text{H}] \quad (1)$$

$$\ln[(\text{diphosphine})\text{Rh}(\text{}^{13}\text{CO})_2\text{H}] = -k_1 t + \ln[(\text{diphosphine})\text{Rh}(\text{}^{13}\text{CO})_2\text{H}]_0 \quad (2)$$

To investigate the possible effect of the natural bite angle on the rate of CO dissociation from the (diphosphine)Rh(CO)₂H complexes, we have synthesized the ¹³CO-labeled complexes for ligands **2**, **4**, and **6**. The (diphosphine)Rh(¹³CO)₂H complexes were prepared in situ from Rh(CO)₂(acac) and diphosphine under an atmosphere of ¹³CO/H₂ (1:4). Complex formation was usually complete within 2 h. The exchange of ¹³CO for ¹²CO in the (diphosphine)Rh(¹³CO)₂H complexes was monitored by rapid-scan HP IR spectroscopy at 40 °C. The ¹³CO/¹²CO exchange was initiated by adding a large excess of ¹²CO (20-fold or more). The strongest carbonyl absorptions of the complexes at approximately 1908 cm⁻¹ were taken to calculate the concentrations of the complexes. These absorption bands, which are assigned to the symmetric CO vibration of the **ea** complex isomers, are the most characteristic and intensive carbonyl vibrations of the (diphosphine)Rh(¹³CO)₂H complexes due to the strong vibrational coupling between the two equatorial ¹³CO ligands. The difference between the **ee** and **ea** isomers of the (diphosphine)Rh(¹³CO)₂H complexes cannot be determined, since the exchange between **ee** and **ea** isomers is several orders of magnitude faster than the rates of ¹³CO dissociation.⁴² Representative kinetic data of the experiments with ligand **2**, **4**, and **6** are shown in Figure 6, and the observed rate constants, *k*₁, are listed in Table 8.

The representative difference IR spectrum displayed in Figure 6a for one of the experiments with (thixantphos)Rh(¹³CO)₂H (**14a-¹³CO**) clearly shows that the ¹³CO-labeled complex is quantitatively converted into its ¹²CO analogue. The exponential decay of the intensity of the strongest carbonyl absorption (1908 cm⁻¹) of complex **14a-¹³CO** versus time is displayed in Figure 6b. The solvent cyclohexane used in the experiment is responsible for the remaining background absorption of 0.71 au. By converting the background-corrected absorbance in the complex concentration the linear plot of the natural logarithm of the complex concentration (ln-

Table 8. Kinetics of ¹³CO Dissociation of (Diphosphine)Rh(¹³CO)₂H Complexes^a

ligand	β _n , deg	P(CO) (bar)	r ²	k ₁ (h ⁻¹)
2	107.9	25	0.998	177 ± 2
2		25	0.999	174 ± 1
4	109.6	25	1.000	206 ± 1
4^b		25	1.000	200 ± 1
6	113.2	20	0.999	182 ± 1
6		25	1.000	185 ± 1
6		30	0.999	181 ± 1

^a Reaction conditions: [(diphosphine)Rh(¹³CO)₂H] = 2.00 mM in cyclohexane, P(¹³CO) = 1 bar, P(H₂) = 4 bar, T = 40 °C, diphosphine/Rh = 5. Values for *k*₁ are least-squares fit of lines from ln[(diphosphine)Rh(¹³CO)₂H] vs time over the first 25 s, calculated using TableCurve 2D.⁴³ ^b [(diphosphine)Rh(¹³CO)₂H] = 3.00 mM.

[**14a-¹³CO**]) versus time can be obtained (Figure 6c). The slope of this line is the negative of the first-order rate constant *k*₁ (eq 2).

The decay of the carbonyl resonances of the (diphosphine)Rh(¹³CO)₂H complexes in time follows simple first-order kinetics in all experiments. Experimental reproducibility is within 3% for duplo experiments, and plots of the ln[(diphosphine)Rh(¹³CO)₂H] versus time are linear for at least 2 half-lives. The *r*² coefficients of the least-squares fits of the lines are more than 0.998. This clearly confirms that re-formation of the (diphosphine)Rh(¹³CO)₂H complex via the *k*₋₁ pathway is suppressed effectively, and all dissociated ¹³CO is replaced by ¹²CO. The experiments with ligand **6** at different ¹²CO partial pressure show that the rate of CO displacement is independent of the CO pressure. Furthermore, the rate is also independent of the (diphosphine)Rh(¹³CO)₂H complex concentration, as demonstrated by the experiments with ligand **4**. It can therefore be concluded that the CO dissociation for these complexes proceeds by a purely dissociative mechanism and obeys a first-order rate-law. Employing the described experimental setup, the rate constants *k*₁ for CO dissociation from the (diphosphine)Rh(CO)₂H complexes are obtained for the first time.

Table 8 shows that there is no correlation between the rate of CO dissociation and the natural bite angle. The rate constants *k*₁ for ligands **2**, **4**, and **6** do not differ significantly and cannot explain the trend in observed hydroformylation activities. The comparison of the *k*₁ values for ligands **2**, **4**, and **6** with the turnover frequencies depicted in Table 4 reveal that the rates of CO dissociation, measured at 40 °C, are higher than the hydroformylation rates at 80 °C. Since reaction rates increase approximately an order of magnitude with a temperature rise of 20 deg, the CO dissociation rate at 80 °C is about 100 times as fast as the hydroformylation reaction.

Discussion

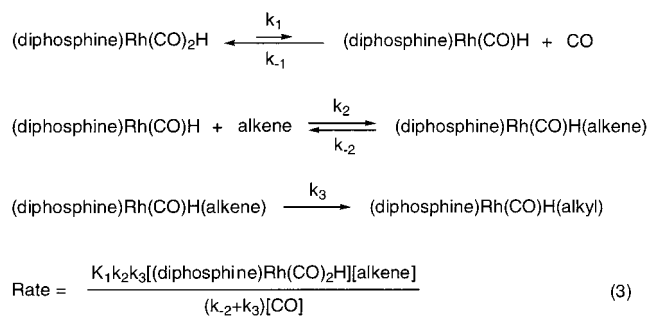
Within the series of xantphos ligands no clear effect of the ligand backbone is found on the bite angles observed in the crystal structures of the (diphosphine)Rh(CO)H(PPh₃) complexes or on the **ee:ea** isomer composition of the (diphosphine)Rh(CO)₂H complexes. These results are in contradiction with studies of Casey and co-workers in which diphosphines with wider natural bite angles have an increased preference for **ee** chelation.^{5,14} Evidently, only for flexible diphosphines

(40) The transient (diphosphine)Rh(¹³CO)(¹²CO)H complex is not observed in the IR experiments. The intensities of the carbonyl absorptions of this complex are considerably lower than those of the isotopically pure complexes due to the absence of vibrational coupling between the CO ligands. Furthermore, *three* complex isomers exist for this complex, which results in even lower intensities of the *six* separate absorption bands.

(41) Cotton, F. A.; Wilkinson, G. *Advanced Inorganic Chemistry*, 5th ed.; Wiley: New York, 1988.

(42) The energy barrier for the interconversion of the two isomers is very low, probably less than 10 kcal mol⁻¹.²⁰

Scheme 4



having either a relatively narrow natural bite angle (dppe) or a relatively wide one (BISBI) does the natural bite angle control the chelation mode.⁵ The rhodium complexes of the more rigid xantphos-type ligands having intermediate natural bite angles prove to be sensitive to small changes in the electronic properties and the rigidity of the ligand backbone. In these complexes the chelation mode is only partially imposed by the natural bite angle. The pronounced effect of phosphine basicity on chelation behavior has been demonstrated before.^{14,20,36}

The natural bite angle does have a clear effect on the selectivity for linear aldehyde formation in the hydroformylation of both 1-octene and styrene. This unambiguously proves that the **ee:ea** isomer ratio in the (diphosphine)Rh(CO)₂H catalyst resting states is not a key parameter controlling regioselectivity. The bite angle effect on regioselectivity has to operate via another mechanism. The expansion of the effective steric bulk of the diphosphine with increasing natural bite angle is the most likely explanation.⁵ Increasing the steric congestion around the rhodium center will result in more selective formation of the sterically less hindered linear rhodium alkyl species. This is consistent with our model suggested previously, in which the four-coordinate intermediate (diphosphine)Rh(CO)H species that undergoes the alkene attack plays an important role in the control of regioselectivity.²⁰ The regioselectivity is finally fixed upon the migration of the hydride to the coordinated alkene (assuming that this step is irreversible).

So far it is unclear in which step of the hydroformylation cycle the bite angle affects the activity. The rate of CO dissociation (k_1) or association (k_{-1}), the rate of alkene coordination (k_2) or dissociation (k_{-2}), and the rate of alkene insertion (k_3) could all be influenced by the bite angle (Scheme 4). Treating the step of CO dissociation/association as a preequilibrium and employing the steady-state approximation for the (diphosphine)Rh(CO)H(alkene) complex leads to eq 3 as the general rate expression for the reaction sequence depicted in Scheme 4.⁴¹ The step of CO dissociation/association can be treated as a preequilibrium, since $k_1[(\text{diphosphine)Rh(CO)}_2\text{H}]$ is orders of magnitude faster than the overall hydroformylation rate and the (diphosphine)Rh(CO)H complex is not observed under hydroformylation conditions or in the CO dissociation studies, indicating that $k_{-1}[\text{CO}]$ is orders of magnitude larger than k_1 and k_2 . The use of the steady-state approximation is justified since the (diphosphine)Rh(CO)H(alkene) complex is also not observed under hydroformylation conditions.

In the present study no influence of the natural bite angle on the rate of formation of the (diphosphine)Rh(CO)H complexes (k_1) is found, implying that the activation energy for the formation of these complexes is not affected significantly. Therefore, the increase in hydroformylation rate with increasing bite angle can originate (i) from an increase in the concentration of this four-coordinate complex, i.e., from a decrease of the rate of CO association (k_{-1}), (ii) from an increase in the rate of alkene coordination (k_2), (iii) from a decrease in the rate of alkene dissociation (k_{-2}), or (iv) from an increase in the rate of alkene insertion (k_3).

What kind of electronic effect the widening of the bite angle has on the activation energy for CO and alkene coordination (k_{-1} and k_2) is unclear, since it depends on the bonding modes of the ligands.⁴⁴ Rhodium to CO/alkene back-donation is promoted by narrow bite angles, while CO/alkene to rhodium donation is enhanced by wide bite angles. Sterically, alkene coordination will experience a much stronger influence of the natural bite angle of the diphosphine than the association of the smaller CO ligand. Increasing the bite angle results in increased steric congestion around the rhodium center and consequently in more steric hindrance for the ligand entering the coordination sphere. This could result in a decrease of k_2 and an increase of k_{-2} . On the basis of the results of the CO dissociation experiments, however, it is not likely that the rate of alkene dissociation (k_{-2}) is affected by the natural bite angle.

The increase of the hydroformylation activity with increasing natural bite angle may be explained by the relative stability of the unsaturated four-coordinate (diphosphine)Rh(CO)H complex.²⁰ In these square-planar complexes trans coordination of the diphosphines is energetically more favorable than cis coordination.⁴⁵ Diphosphines that can accommodate the wide bite angles required for the formation of the trans square-planar complexes will therefore lead to more stable (diphosphine)Rh(CO)H complexes. The concentration of the four-coordinate complexes is directly related to the relative stability of these complexes compared to the five-coordinate (diphosphine)Rh(CO)₂H complexes. In rate equation 3 (Scheme 4) the relative stability of the four-coordinate complexes is reflected in the equilibrium constant for CO dissociation K_1 . Since the natural bite angle has no regular effect on k_1 , according to this explanation, increasing the bite angle will have to result in a decrease of rate constant k_{-1} , leading to an increase of K_1 .

Another explanation for the origin of the bite angle effect on the activity in hydroformylation is found in the increase of the rate of alkene insertion (k_3). Theoretical studies on platinum-hydride complexes have shown that upon alkene insertion the P–Pt–P bite angle increases.^{46,47} On the basis of these results it can be concluded that widening of the natural bite angle enhances the alkene insertion reaction and, therefore, can increase the hydroformylation rate. The influence

(43) TableCurve, Jandel Scientific.

(44) Li, J.; Schreckenbach, G.; Ziegler, T. *Inorg. Chem.* **1995**, *34*, 3245–3252.(45) Schmid, R.; Herrmann, W. A.; Frenking, G. *Organometallics* **1997**, *16*, 701–708.(46) Thorn, D. L.; Hoffmann, R. *J. Am. Chem. Soc.* **1978**, *100*, 2079.(47) Rocha, W. R.; De Almeida, W. B. *Organometallics* **1998**, *17*, 1961–1967.

of the natural bite angle on the rate of CO insertion has already been demonstrated both experimentally and theoretically.^{48–50}

For styrene a somewhat different trend in the activity is observed than for 1-octene. This may be explained by a shift of the rate-limiting step in the ligand series.⁵¹ For now it is still unclear what causes the decrease of the activity with increasing natural bite angle in the first half of the ligand series. The increase in activity with increasing natural bite angle in the latter half of the ligand series can be explained along the same lines as for 1-octene; that is, the formation of the (diphosphine)Rh(CO)H complexes and/or alkene insertion can be favored by wider natural bite angles.

Conclusion

No distinct effect of the natural bite angle on the coordination mode in the (diphosphine)Rh(CO)H(PPh₃) and (diphosphine)Rh(CO)₂H complexes within the series of xantphos-type ligands was found. Although benzoxantphos has a 10° wider calculated natural bite angle than thixantphos, the observed bite angle in the (benzoxantphos)Rh(CO)H(PPh₃) (**19a**) complex is even smaller than that of thixantphos in the corresponding complex (**14a**). For the (diphosphine)Rh(CO)₂H complexes wider natural bite angles do not lead to increased *ee:ea* isomer ratios. The natural bite angle, however, does affect the catalytic performance of the xantphos-type ligands. In the hydroformylation of both 1-octene and styrene the bite angle correlates well with the *selectivity* for linear aldehyde formation. The same trend is also valid for the *activity* in 1-octene hydroformylation and to a certain extent in styrene hydroformylation. The bite angle effect on selectivity originates from the steps of alkene coordination and hydride migration. The increase in steric congestion around the rhodium center upon widening the bite angle leads to more selective formation of the sterically less demanding linear alkyl rhodium species.

It is still unclear how the bite angle influences the activity in the catalytic cycle. Both the equilibrium constant for CO dissociation and the rate of alkene insertion could be affected. For the first time we have determined the rate constants for CO dissociation from (diphosphine)Rh(CO)₂H complexes using rapid-scan FT IR spectroscopy. The kinetic experiments with three (diphosphine)Rh(CO)₂H complexes show that the bite angle has no regular effect on CO dissociation rates and that the CO dissociation is approximately 100 times as fast as the hydroformylation reaction. We suggest that the bite angle effect on the activity in the hydroformylation with xantphos-type ligands is caused by the decrease of the CO association rate, resulting in an increase of the concentration of the intermediate four-coordinate (diphosphine)Rh(CO)H complexes or by an increase of the rate of alkene insertion. In this context it has to be noted that the ability of the ligand to encompass the whole range of bite angles associated with the different rhodium species in the hydroformy-

lation cycle may be more important than the absolute value of the natural bite angle. Since the four-coordinate (diphosphine)Rh(CO)H complexes have escaped direct observation so far, we are currently, in collaboration with Dr. C. Bo from the Universitat Rovira i Virgili in Tarragona, performing theoretical calculations using density functional theory to further clarify the effect of the bite angle of xantphos-type ligands on these complexes.

Experimental Section

Computational Details. The molecular mechanics calculations were performed using the CAChe WorkSystem version 4.0.⁵² on a Apple Power Macintosh 950, equipped with two CAChe CXP coprocessors. Calculations were carried out similarly to the method described by Casey and Whiteker,²⁴ using a Rh–P bond length of 2.315 Å. Minimizations were done using the block-diagonal Newton–Raphson method, allowing the structures to converge with a termination criterion of a rms factor of 0.0001 kcal mol⁻¹ Å⁻¹ or less.

General Procedure. All reactions were carried out using standard Schlenk techniques under an atmosphere of purified argon. Toluene and TMEDA were distilled from sodium, THF and diethyl ether from sodium/benzophenone, and hexanes from sodium/benzophenone/triglym. Methanol, ethanol, and dichloromethane were distilled from CaH₂. Chemicals were purchased from Acros Chimica and Aldrich Chemical Co. (PPh₃)₃Rh(CO)H,⁵³ 10,11-dihydrodibenzo[*b,f*]oxepine,²⁸ 10-phenylphenoxaphosphine,²⁹ 9-(*tert*-butyldimethylsilyl)phenoxazine,³⁰ and benzo[*k,l*]xanthene^{31,54} were prepared according to literature procedures. Silica gel 60 (230–400 mesh) purchased from Merck was used for column chromatography. Melting points were determined on a Gallenkamp MFB-595 melting point apparatus in open capillaries and are uncorrected. NMR spectra were obtained on a Bruker AMX 300 spectrometer. ³¹P and ¹³C spectra were measured ¹H decoupled. TMS was used as an internal standard for ¹H and ¹³C NMR and H₃PO₄ for ³¹P NMR. Mass spectroscopy was measured on a JEOL JMS-SX/SX102A. Elemental analyses were carried out on an Elementar Vario EL apparatus. Standard infrared spectra were recorded on a Nicolet 510 FT IR spectrophotometer, and rapid-scan (4.5 spectra per second) measurements were performed using a Bio-Rad FTS-60A spectrophotometer. HP IR spectra were measured using a 20 mL homemade stainless steel autoclave equipped with mechanical stirring and ZnS windows. Hydroformylation reactions were carried out in a 200 mL homemade stainless steel autoclave. Syn gas (CO/H₂, 1:1, 99.9%) and CO (99.9%) were purchased from Air Liquide. D₂ was purchased from Hoekloos. ¹³CO (99%) was purchased from Cambridge Isotope Laboratories. Gas chromatographic analyses were run on an Interscience HR GC Mega 2 apparatus (split/splitless injector, J&W Scientific, DB1 30m column, film thickness 3.0 mm, carrier gas 70 kPa He, FID detector) equipped with a Hewlett-Packard data system (Chrom-Card).

10-Isopropylidenexanthene (10).³² A 7.0 g sample of freshly flattened lithium metal (1.0 mol) was added to a suspension of 44.5 g of titanium chloride (288 mmol) in 300 mL of 1,2-dimethoxyethane. The reaction mixture was heated at reflux temperature for 1 h. After cooling to room temperature, 8.09 g of xanthone (41.2 mmol) and 3.03 mL of acetone (41.2 mmol) were added, and the reaction mixture was heated at reflux temperature for another 22 h. The reaction mixture was diluted with 250 mL of light petroleum ether, filtered over Celite, and concentrated to give a brown oil. The product was

(48) Anderson, G. K.; Lumetta, G. J. *Organometallics* **1985**, *4*, 1542–1545.

(49) Dekker, G. P. C. M.; Elsevier, C. J.; Vrieze, K.; van Leeuwen, P. W. N. M. *Organometallics* **1992**, *11*, 1598–1603.

(50) Koga, N.; Morokuma, K. *Chem. Rev.* **1991**, *91*, 823–842.

(51) van Rooy, A.; Orij, E. N.; Kamer, P. C. J.; van Leeuwen, P. W. N. M. *Organometallics* **1995**, *14*, 34–43.

(52) CAChe Scientific Inc., 18700 N.W. Walker Road, Building 92-01, Beaverton, OR 97006.

(53) Ahmad, N.; Levison, J. J.; Robinson, S. D.; Uttley, M. F. *Inorg. Synth.* **1974**, *15*, 59–60.

(54) Rice, J. E.; Cai, Z.-W. *Tetrahedron Lett.* **1992**, *33*, 1675–1678.

purified by column chromatography (5% toluene in light petroleum ether (v:v), $R_f = 0.28$). Yield: 5.63 g of a light yellow oil (61%) that slowly crystallized. Mp: 78–80 °C. ^1H NMR (CDCl_3): $\delta = 7.37$ (dd, $^3J(\text{H,H}) = 7.7$ Hz, $^4J(\text{H,H}) = 1.5$ Hz, 2H; CH), 7.26 (m, 4H; CH), 7.18 (dt, $^3J(\text{H,H}) = 7.0$ Hz, $^4J(\text{H,H}) = 2.3$ Hz, 2H; CH), 2.18 (s, 6H; CH_3). $^{13}\text{C}\{^1\text{H}\}$ NMR (CDCl_3): $\delta = 154.1$ (CO), 130.5, 128.3 (CH), 127.0 (CH), 126.7, 122.5, 122.2 (CH), 116.1 (CH), 23.0 (CH_3). IR (KBr, cm^{-1}): 3071 (w), 2939 (w), 2907 (w), 1472 (m), 1448 (s), 1255 (s), 1213 (m), 1197 (m), 755 (s). GC-MS (m/z , rel intensity): 222 (M^+ , 100), 221 (84), 207 (68), 181 (21), 178 (15), 152 (12), 110 (9.9), 103 (9.7). Anal. Calcd for $\text{C}_{16}\text{H}_{14}\text{O}$: C, 86.45; H, 6.35. Found: C, 86.25; H, 6.58. Exact mass (MS): 223.1160 ($\text{M} + \text{H}$) (calcd for $\text{C}_{16}\text{H}_{15}\text{O}$ 223.1123).

Xantphos-Type Ligands 1–9. In a typical experiment, 6.1 mL of *n*-butyllithium (2.5 M in hexanes, 15 mmol) was added dropwise to a stirred solution of 1.0 mL of 10,11-dihydro-dibenzo[*b*,*f*]oxepine²⁸ (6.1 mmol) and 2.3 mL of TMEDA (15 mmol) in 25 mL of diethyl ether at 0 °C. The reaction mixture was slowly warmed to room temperature and stirred for 16 h. The orange suspension was cooled to 0 °C, and a solution of 3.0 mL of chlorodiphenylphosphine (17 mmol) in 10 mL of hexanes was added dropwise. The reaction mixture decolorized, and a beige precipitate was formed. After being stirred for 16 h at room temperature, the reaction mixture was diluted with 50 mL of THF and hydrolyzed with 25 mL of a 1:1 mixture of brine and dilute hydrochloric acid. The water layer was removed, and the organic layer was dried over MgSO_4 . The solvent was removed in vacuo, and the resulting residue was washed with 25 mL of hexanes and crystallized from dichloromethane/EtOH. Yield: 2.75 g of pure white crystals of homoxantphos (**1**, 80%). All xantphos-type ligands **1–9** were fully characterized.^{55–57} Detailed descriptions of the syntheses and characterizations are included in the Supporting Information.

(Homoxantphos)Rh(CO)H(PPh₃) (11a). A solution of $(\text{PPh}_3)_3\text{Rh}(\text{CO})\text{H}$ (92 mg, 0.10 mmol) and **1** (62 mg, 0.11 mmol) in 5 mL of dichloromethane was stirred for 1 h at room temperature. The solvent was removed in vacuo, and the resulting yellow solid was washed with methanol. ^1H NMR (C_6D_6): $\delta = 7.78$ (bs, 10H; CH), 7.51 (bs, 4H; CH), 7.02 (bs, 10H; CH), 6.91 (m, 11H; CH), 6.77 (m, 2H; CH), 6.70 (d, $^3J(\text{H,H}) = 6.3$ Hz, 2H; $\text{H}^{1,8}$), 6.57 (m, 2H; CH), 2.66 (s, 4H; CH_2), -9.05 (td, $^1J(\text{Rh,H}) = 16.5$ Hz, $^2J(\text{P,H}) = 9.8$ Hz, 1H; RhH). $^{31}\text{P}\{^1\text{H}\}$ NMR (C_6D_6): $\delta = 44.5$ (td, $^1J(\text{Rh,P}) = 165.2$ Hz, $^2J(\text{P,P}) = 117.7$ Hz; PPh_3), 28.0 (dd, $^1J(\text{Rh,P}) = 146.3$ Hz, $^2J(\text{P,P}) = 117.7$ Hz, 2P). IR (KBr, carbonyl region, cm^{-1}): 1982 (vs, HRhCO), 1921 (w, HRhCO).

(Homoxantphos)Rh(CO)₂H (11b). A solution of $\text{Rh}(\text{CO})_2\text{-}(\text{acac})$ (2.6 mg, 10 μmol) and **1** (6.2 mg, 11 μmol) in 1.0 mL of C_6D_6 was pressurized with 20 bar of CO/H_2 (1:1) and stirred for 2 h at 70 °C. After being cooled to room temperature, the reaction mixture was depressurized and transferred into a 0.5 cm NMR tube and directly analyzed at atmospheric pressure. ^1H NMR (C_6D_6): $\delta = 7.85$ (bm, 2H; CH), 7.50 (m, 6H; CH), 7.04 (bs, 4H; CH), 6.90 (bm, 8H; CH), 6.76 (bm, 4H; CH), 6.57 (m, 2H; CH), 6.68 (t, $^3J(\text{H,H}) = 7.7$ Hz, 2H; CH), 6.58 (m, 2H; CH), 2.72 (m, 4H; CH_2), -8.28 (dt, $^1J(\text{Rh,H}) = 9.5$ Hz, $^2J(\text{P,H})$

$= 37.7$ Hz, 1H; RhH). $^{31}\text{P}\{^1\text{H}\}$ NMR (C_6D_6): $\delta = 24.7$ (d, $^1J(\text{Rh,P}) = 120.3$ Hz). HP IR (cyclohexane, carbonyl region, cm^{-1}): 2040 (RhCO), 1997 (RhCO), 1974 (RhCO), 1951 (RhCO).

(Phosxantphos)Rh(CO)H(PPh₃) (12a). This compound was prepared similarly to **11a**. IR (KBr, carbonyl region, cm^{-1}): 1966 (s, HRhCO), 1925 (m, HRhCO).

(Phosxantphos)Rh(CO)₂H (12b). This compound was prepared similarly to **11b**. ^1H NMR (C_6D_6): $\delta = 7.75$ (bm, 4H; CH), 7.38 (bm, 4H; CH), 6.78 (bm, 23H; CH), -8.55 (dt, $^1J(\text{Rh,H}) = 7.0$ Hz, $^2J(\text{P,H}) = 17.0$ Hz, 1H; RhH). $^{31}\text{P}\{^1\text{H}\}$ NMR (C_6D_6): $\delta = 22.8$ (d, $^1J(\text{Rh,P}) = 126.5$ Hz). HP IR (cyclohexane, carbonyl region, cm^{-1}): 2040 (RhCO), 1999 (RhCO), 1977 (RhCO), 1953 (RhCO).

(Isopropxantphos)Rh(CO)H(PPh₃) (16a). This compound was prepared similarly to **11a**. ^1H NMR (C_6D_6): $\delta = 7.83$ (quar., $^3J(\text{H,H}) = 4.5$ Hz, $^3J(\text{P,H}) = 4.5$ Hz, 4H; CH), 7.61 (m, 6H; CH), 7.50 (bs, 4H; CH), 7.17 (m, 2H; CH), 6.90 (m, 21H; CH), 6.72 (m, 4H; CH), 1.79 (s, 6H; CH_3), -9.05 (bm, 1H; RhH). $^{31}\text{P}\{^1\text{H}\}$ NMR (C_6D_6): $\delta = 41.8$ (td, $^1J(\text{Rh,P}) = 166.9$ Hz, $^2J(\text{P,P}) = 132.4$, 1P; PPh_3), 25.17 (dd, $^1J(\text{Rh,P}) = 148.6$ Hz, $^2J(\text{P,P}) = 131.9$ Hz, 2P). IR (KBr, carbonyl region, cm^{-1}): 1990 (vs, HRhCO), 1920 (m, HRhCO). Anal. Calcd for $\text{C}_{59}\text{H}_{48}\text{O}_2\text{P}_3\text{-Rh}$: C, 71.95; H, 4.92. Found: C, 71.40; H, 5.13.

(Isopropxantphos)Rh(CO)₂H (16b). This compound was prepared similarly to **11b**. ^1H NMR (C_6D_6): $\delta = 7.61$ (bm, 8H; CH), 7.16 (dd, $^3J(\text{H,H}) = \text{unresolved}$, $^4J(\text{H,H}) = 1.5$ Hz, 2H; CH), 6.86 (bm, 12H; CH), 6.68 (t, $^3J(\text{H,H}) = 7.7$ Hz, 2H; CH), 6.58 (m, 2H; CH), -8.60 (dt, $^1J(\text{Rh,H}) = 6.2$ Hz, $^2J(\text{P,H}) = 13.0$ Hz, 1H; RhH). $^{31}\text{P}\{^1\text{H}\}$ NMR (C_6D_6): $\delta = 23.5$ (d, $^1J(\text{Rh,P}) = 128.3$ Hz). HP IR (cyclohexane, carbonyl region, cm^{-1}): 2041 (RhCO), 1999 (RhCO), 1976 (RhCO), 1952 (RhCO).

(Isopropxantphos)Rh(CO)(¹³CO)H (16b-¹³CO). $^{13}\text{C}\{^1\text{H}\}$ HP NMR (323 K, 18 bar CO/H_2 (1:1), 2 bar ^{13}CO , C_6D_6): $\delta = 199.8$ (bd, $^1J(\text{Rh,C}) = 65.3$ Hz; Rh- ^{13}CO).

(Benzylnixantphos)Rh(CO)H(PPh₃) (17a). This compound was prepared similarly to **11a**. ^1H NMR (C_6D_6): $\delta = 7.80$ (m, 8H; CH), 7.59 (m, 6H; CH), 7.47 (bs, 4H; CH), 6.91 (m, 22H; CH), 6.35 (m, 4H; CH), 6.23 (d, $^3J(\text{H,H}) = 7.5$ Hz, 2H; CH), 4.46 (s, 2H; CH_2), -9.06 (td, $^1J(\text{Rh,H}) = 18.6$ Hz, $^2J(\text{P,H}) = 12.7$ Hz, 1H; RhH). $^{31}\text{P}\{^1\text{H}\}$ NMR (C_6D_6): $\delta = 42.0$ (dt, $^1J(\text{Rh,P}) = 167.1$ Hz, $^2J(\text{P,P}) = 132.7$, 1P; PPh_3), 25.17 (dd, $^1J(\text{Rh,P}) = 148.4$ Hz, $^2J(\text{P,P}) = 132.6$ Hz, 2P). IR (KBr, carbonyl region, cm^{-1}): 2000 (vs, HRhCO), 1920 (m, HRhCO).

(Benzylnixantphos)Rh(CO)₂H (17b). This compound was prepared similarly to **11b**. ^1H NMR (C_6D_6): $\delta = 7.63$ (m, 8H; CH), 7.00 (m, 12H; CH), 6.27 (m, 6H; CH), 4.46 (s, 2H; CH_2), -8.62 (dt, $^1J(\text{Rh,H}) = 6.0$ Hz, $^2J(\text{P,H}) = 13.0$ Hz, 1H; RhH). $^{31}\text{P}\{^1\text{H}\}$ NMR (C_6D_6): $\delta = 20.2$ (d, $^1J(\text{Rh,P}) = 127.6$ Hz). HP IR (cyclohexane, carbonyl region, cm^{-1}): 2040 (RhCO), 1999 (RhCO), 1977 (RhCO), 1953 (RhCO).

(Nixantphos)Rh(CO)H(PPh₃) (18a). This compound was prepared similarly to **11a**. Yellow crystals suitable for X-ray structure determination were obtained from toluene/ethanol. ^1H NMR (C_6D_6): $\delta = 7.76$ (quar., $^3J(\text{H,H}) = 5.9$ Hz, $^3J(\text{P,H}) = 5.9$ Hz, 4H; CH), 7.58 (m, 6H; CH), 7.47 (bs, 4H; CH), 6.89 (m, 21H; CH), 6.54 (t, $^3J(\text{H,H}) = 7.8$ Hz, 2H; $\text{H}^{2,7}$), 6.38 (m, 2H; $\text{H}^{3,6}$), 6.08 (d, $^3J(\text{H,H}) = 7.5$ Hz, 2H; $\text{H}^{1,8}$), 4.52 (s, 1H; NH), -9.17 (td, $^1J(\text{Rh,H}) = 19.8$ Hz, $^2J(\text{P,H}) = 12.1$ Hz, 1H; RhH). $^{31}\text{P}\{^1\text{H}\}$ NMR (C_6D_6): $\delta = 41.1$ (bquar., $^1J(\text{Rh,P}) = 141$ Hz, $^2J(\text{P,P}) = 141$, 1P; PPh_3), 28.0 (bt, $^1J(\text{Rh,P}) = 137$ Hz, $^2J(\text{P,P}) = 137$ Hz, 2P). IR (KBr, carbonyl region, cm^{-1}): 1988 (vs, HRhCO), 1920 (m, HRhCO). Anal. Calcd for $\text{C}_{55}\text{H}_{43}\text{NO}_2\text{P}_3\text{Rh}$: C, 69.85; H, 4.59; N, 1.48. Found: C, 67.37; H, 4.65; N, 1.46.

X-ray Crystal Structure Determination of 18a. **18a** crystallized in the triclinic space group $P\bar{1}$, $a = 13.0018(6)$ Å, $b = 14.2404(7)$ Å, $c = 16.2583(9)$ Å, $\alpha = 64.041(3)^\circ$, $\beta = 78.834(3)^\circ$, $\gamma = 80.269(2)^\circ$, $V = 2643.3(2)$ Å³, and $Z = 1$. The data collection was carried out at 230 K. The structure was solved by direct methods. The hydrogen atoms were calculated. The structure was refined to $R = 0.0363$ and $R_w = 0.0827$, for 8443 observed reflections. Crystal data and collection parameters,

(55) Unfortunately, no satisfying elemental analysis could be obtained for compound **7**. However, the molecular formula of **7** is confirmed by exact mass determination and multinuclear NMR spectroscopy. ^1H , $^{31}\text{P}\{^1\text{H}\}$, and $^{13}\text{C}\{^1\text{H}\}$ NMR spectra of **7** are included in the Supporting Information.

(56) Complexes **11a**, **12a**, and **16a–19a** were made for spectroscopic purposes only; hence, no yields were determined. No satisfactory elemental analyses could be obtained for complexes **11a**, **12a**, **17a**, and **18a**, since we were unable to strip these complexes from excess triphenylphosphine and/or solvent, without losing structural integrity. ^1H and $^{31}\text{P}\{^1\text{H}\}$ NMR spectra of the complexes are included in the Supporting Information.

(57) Complexes **11b–19b** are stable only under an atmosphere of CO and H_2 . ^1H and $^{31}\text{P}\{^1\text{H}\}$ NMR spectra of the complexes **11b**, **12b**, and **16b–19b** are included in the Supporting Information.

atomic coordinates, bond lengths, bond angles, and thermal parameters are included in the Supporting Information.

(Nixantphos)Rh(CO)₂H (18b). This compound was prepared similarly to **11b**. ¹H NMR (C₆D₆): δ = 7.61 (bs, 4H; CH), 7.52 (bm, 2H; CH), 6.89 (bm, 14H; CH), 6.51 (t, ³J(H,H) = 7.5 Hz, 2H; H^{2,7}), 6.26 (m, 2H; H^{3,6}), 6.12 (dd, ³J(H,H) = 7.8 Hz, ⁴J(H,H) = 1.2 Hz, 2H; CH), 4.62 (bs, 1H; NH), -8.69 (dt, ¹J(Rh,H) = 6.1 Hz, ²J(P,H) = 14.5 Hz, 1H; RhH). ³¹P{¹H} NMR (C₆D₆): δ = 19.8 (d, ¹J(Rh,P) = 127.2 Hz). HP IR (cyclohexane, carbonyl region, cm⁻¹): 2038 (RhCO), 1997 (RhCO), 1977 (RhCO), 1951 (RhCO).

(Benzoxantphos)Rh(CO)H(PPh₃) (19a). This compound was prepared similarly to **11a**. Red crystals suitable for X-ray structure determination were obtained from toluene/ethanol. ¹H NMR (C₆D₆): δ = 7.75 (t, ³J(H,H) = 9.4 Hz, 1H; CH), 7.65 (t, ³J(H,H) = 8.7 Hz, 1H; CH), 7.52 (m, 6H; CH), 7.25 (dd, ²J(P,H) = 11.7 Hz, ³J(H,H) = 7.6 Hz, 1H; PCCH), 6.91 (m, 19H; CH), 6.70 (t, ³J(H,H) = 7.5 Hz, 1H; CH), -9.23 (td, ¹J(Rh,H) = 18.9 Hz, ²J(P,H) = 12.3 Hz, 1H; RhH). ³¹P{¹H} NMR (C₆D₆): δ = 42.1 (dt, ¹J(Rh,P) = 170.0 Hz, ²J(P,P) = 142.9 Hz, PPh₃), 21.8 (AB-system: δ_A = 21.8 (t, ¹J(Rh,P) = 147.5 Hz, ²J(P,P) = 147.5 Hz), δ_B = 19.2 (t, ¹J(Rh,P) = 142.9 Hz, ²J(P,P) = 142.9 Hz), J_{AB} = 77.3 Hz, 2P). IR (KBr, carbonyl region, cm⁻¹): 1989 (vs, HRhCO), 1919 (m, HRhCO). Anal. Calcd for C₅₉H₄₄O₂P₃Rh: C, 72.25; H, 4.52. Found: C, 72.17; H, 4.71.

X-ray Crystal Structure Determination of 19a. **19a** crystallized in the monoclinic space group *P*2₁/*c*, *a* = 25.3330(6) Å, *b* = 18.7936(5) Å, *c* = 11.7296(2) Å, α = 90°, β = 92.6944(14)°, γ = 90°, *V* = 5578.3(2) Å³, and *Z* = 4. The data collection was carried out at 150 K. The structure was solved by direct methods. The hydrogen atoms were calculated. The structure was refined to *R* = 0.0590 and *R*_w = 0.1237, for 6496 observed reflections. Crystal data and collection parameters, atomic coordinates, bond lengths, bond angles, and thermal parameters are included in the Supporting Information.

(Benzoxantphos)Rh(CO)₂H (19b). This compound was prepared similarly to **11b**. ¹H NMR (C₆D₆): δ = 7.58 (quar., ³J(H,H) = 10.1 Hz, ³J(P,H) = 10.1 Hz, 4H; CH), 7.40 (m, 6H; CH), 7.24 (m, 4H; CH), 7.00 (m, 11H; CH), 6.70 (m, 3H; CH), -8.74 (ddd, ¹J(Rh,H) = 7.1 Hz, ²J(P,H) = 24.8 Hz, ²J(P,H) = 18.3 Hz, 1H; RhH). ³¹P{¹H} NMR (C₆D₆): δ = 16.4 (dd, ¹J(Rh,P) = 122.2 Hz, ²J(P,P) = 20.8 Hz, 1P), 13.1 (dd, ¹J(Rh,P) = 122.2 Hz, ²J(P,P) = 21.0 Hz, 1P). HP IR (cyclohexane, carbonyl region, cm⁻¹): 2036 (RhCO), 1996 (RhCO), 1977 (RhCO), 1967 (RhCO).

Hydroformylation Experiments. Hydroformylation reactions were carried out in an autoclave, equipped with a glass inner beaker, a substrate inlet vessel, a liquid sampling valve, and a magnetic stirring rod. The temperature was controlled by an electronic heating mantle. In a typical experiment the

desired amount of ligand was placed in the autoclave, and the system was evacuated and heated to 50 °C. After 0.5 h the autoclave was filled with CO/H₂ (1:1) and a solution of Rh-(CO)₂(acac) (5 or 10 μmol) in 8.5 mL of toluene. The autoclave was pressurized to the appropriate pressure (6 or 16 bar), heated to the reaction temperature, and stirred for 0.5 h (120 °C) or 1.5 h (80 °C) to form the active catalyst. Then 1.0 mL of substrate (filtered over neutral activated alumina to remove peroxide impurities) and 0.5 mL of the internal standard *n*-decane were placed in the substrate vessel, purged with 10 bar CO/H₂ (1:1), and pressed into the autoclave with 10 or 20 bar CO/H₂ (1:1). At the 20% conversion level the reaction was stopped by adding 0.25 mL of tri-*n*-butyl phosphite and cooling on ice. Samples of the reaction mixture were analyzed by temperature-controlled gas chromatography.

HP FT IR Experiments. In a typical experiment the HP IR autoclave was filled with 2–5 equiv of ligand, 4 mg of Rh-(CO)₂(acac), and 15 mL of cyclohexane. The autoclave was purged three times with 15 bar CO/H₂ (1:1), pressurized to approximately 18 bar, and heated to 80 °C. Catalyst formation was monitored in time by FT-IR and was usually completed within 1 h.

Rapid-Scan HP FT IR Experiments. In a typical experiment the HP IR autoclave was filled with 75 μmol of ligand, 30 or 45 μmol of Rh(CO)₂(acac), and 15 mL of cyclohexane. The autoclave was purged four times with 15 bar of H₂, pressurized to 3 bar with ¹³CO, and consequently to 10 bar with H₂, and heated at 40 °C for approximately 2 h. Next a gas reservoir containing 50 bar of unlabeled CO is opened, which resulted in a total pressure in the autoclave of 30 bar. At the same time the rapid-scan FT IR experiment (53 scans min⁻¹ for a total acquisition time of 2.5 min) is started.

Acknowledgment. Financial support from the Technology Foundation (STW) of the Netherlands Organization for Scientific Research (NWO) is gratefully acknowledged, and we thank J. van Slageren for his assistance with the rapid-scan FT IR experiments.

Supporting Information Available: Detailed description of the syntheses and characterizations of the xantphos-type ligands **1**, **2**, **6–9**, ¹H, ³¹P{¹H}, and ¹³C{¹H} NMR spectra of **7**, ¹H and ³¹P{¹H} NMR spectra of complexes **11a**, **12a**, **17a**, **18a** and complexes **11b**, **12b**, **16b–19b**, preliminary kinetic results of the hydroformylation of 1-octene with ligand **4**, and tables of crystal data and collection parameters, atomic coordinates, bond lengths, bond angles, thermal parameters, and H atom coordinates for **18a** and **19a**. This material is available free of charge via the Internet at <http://pubs.acs.org>.

OM9907340